American Mineralogist, Volume 88, pages 1271–1278, 2003

Chromian spinel during melting experiments of dry peridotite (KLB-1) at 1.0–2.5 GPa

KYOKO N. MATSUKAGE[1,]* AND KEIKO KUBO[2]

[1]Department of Environmental Sciences, Faculty of Sciences, Ibaraki University, 2-1-1 Bunkyo, Mito, Ibaraki 310-0056, Japan
[2]Magma Factory, Earth and Planetary Sciences, Tokyo Institute of Technology, 2-12-1 Ookayama, Meguro-ku, Tokyo 152-8551, Japan

ABSTRACT

The stability and chemistry of chromian spinel were determined for dry mantle (spinel lherzolite) melting at pressures between 1.0 and 2.5 GPa and temperatures between 1250 and 1500 °C. To find the most suitable sample container, we tested three different possibilities at 1.5 GPa: a Pt capsule, a Re/Pt capsule, and a graphite/Pt capsule. The oxygen fugacity of the run products with Pt, Re/Pt, and graphite/Pt are FMQ + 4 to 5, –2 to 0, and < –10, respectively. We conclude that the Re/Pt capsule is most suitable for melting experiments of dry peridotite at high temperatures and the oxygen fugacity similar to that of the terrestrial upper mantle, which has been estimated to be near FMQ. Using Re/Pt capsules, batch-melting experiments of a dry spinel lherzolite from Kilborne Hole (KLB-1) were performed. Our experimental results and natural mantle peridotites are significantly different in terms of the stability field and the Cr/(Cr + Al) atomic ratio (= Cr') of chromian spinel. Spinel, which is common in natural mantle peridotite regardless of their bulk chemistry, disappeared at a much lower degree of melting in our experiments. The upper limit of the Cr' of spinel just before its disappearance decreases rapidly from 0.45 to 0.13 with increasing pressure, whereas natural peridotites have a wide range of Cr' from 0.1 to 0.8. Our dry experiments, compared with previous hydrous experiments, indicate that the upper limit of Cr' increases with increasing H_2O content. These findings suggest that the petrological variation of natural mantle peridotite cannot be formed by simple batch melting but may be the result of more complex melting.

INTRODUCTION

Although it is present only in small quantities, chromian spinel is a very important phase during melting processes in the shallow mantle. The compositional variation of spinel as a function of bulk peridotite chemistry has been well documented in many studies on the basis of field observations (e.g., Dick 1977; Dick and Bullen 1984; Arai 1987, 1990; Takahashi N. 1992; Ozawa 1997). The most important feature of spinel is the wide range of Cr/(Cr + Al) atomic ratio (= Cr'), which rises from 0.05 to 0.6, sometimes reaching 0.8, as the Mg/(Mg + Fe) atomic ratio (= Mg') of coexisting olivine is increased. In natural peridotites, the modal proportion of clinopyroxene gradually decreases and finally disappears with an increase in the Cr' of spinel. The systematic increase in Cr' of spinel is considered to have resulted from partial melting and melt-extraction processes because the partial melting preferentially exhausts clinopyroxene relative to coexisting minerals. Chromian spinel exists in minor amounts throughout the peridotite lithologies: lherzolite, harzburgite, and dunite. Therefore, chromian spinel is considered to be one of the best indicators of degree of partial melting for natural mantle peridotites. The purpose of our study was to determine the chemistry of chromian spinel by melting experiments of KLB-1 (a dry spinel lherzolite from Kilborne Hole) at the conditions of the Earth's uppermost mantle and to evaluate the observations on natural peridotites.

Constraining the chemistry of chromian spinel in high-pressure melting experiments involves at least two experimental difficulties. The first problem is the difficulty in maintaining the proper oxygen fugacity. The composition and stability field of chromian spinel are very sensitive to oxygen fugacity (Roeder and Reynolds 1991). The oxygen fugacity of the upper mantle has been estimated to be about that of the Fayalite-Magnetite-Quartz buffer (= FMQ) (e.g., Mattioli and Wood 1986). Therefore, we have to keep the oxygen fugacity of the run products close to the FMQ buffer during experiments. The containers used by previous workers, however, cannot maintain this redox state, as will be shown later.

The second problem is Fe loss. It is well known that the proportion of Fe transferred from the sample charge to a metal container can be considerable in high-temperature experiments, such as melting of dry peridotite at mantle conditions (e.g., Jaques and Green 1980). Partial melts particularly enhance the Fe loss because of their rapid diffusion of elements. To prevent this effect, many materials have been used. A Pt capsule is refractory enough to conduct the high-temperature experiments, but the amount of Fe lost from silicate melts becomes very significant at high temperatures (e.g., Jaques and Green 1980). Au-Pd, Ag-Pd alloys, Au, and Fe-saturated Pt are less reactive with Fe (e.g., Sisson and Grove 1993; Kawamoto and Hirose 1994; Hirose and Kawamoto 1995; Gaetani and Grove 1998 and references therein), but the melting points of these materials are too low to allow their use in the melting of refractory dry peridotites. At present, a graphite sleeve is generally used as the inner capsule, which is encased in a sealed Pt tube to eliminate Fe-loss in high-temperature experiments (e.g., Kogiso et al. 1998; Takahashi et al. 1998; Walter 1998).

In this paper, we have tested Pt and graphite/Pt capsules as well as a Re/Pt capsule (Re foil as an inner capsule in a sealed Pt tube; Takahashi et al. 1993) and show that Re/Pt makes the

---

* E-mail: kmatsu@mx.ibaraki.ac.jp

most suitable container for melting experiments of dry mantle peridotites. Using the Re/Pt capsule, we report for the first time the systematic chemical variation of chromian spinel during partial melting of KLB-1.

EXPERIMENT FOR EVALUATION OF RE/PT SAMPLE CONTAINER

Experimental procedures

A mineral powder of KLB-1, a natural spinel lherzolite from Kilborne Hole, was used as the starting material. KLB-1 is a fertile peridotite with a composition similar to pyrolite (Takahashi 1986). The powder was ground under acetone in an agate mortar and then dried inside a 1-atm furnace at 1000 °C, with oxygen fugacity controlled at the NNO~FMQ buffer using a CO_2/H_2 gas mixture. The dried sample was stored in glass vials in a 110 °C oven. The Re container (inner diameter 1.4 mm) was made from a Re foil (0.025 mm in thickness). The Re and graphite containers were encased in sealed Pt tubes (1.8 mm inner diameter and 0.2 mm thickness). The Pt single capsule was also sealed.

Melting experiments were performed at a pressure of 1.5 GPa, at temperatures of 1375 and 1425 °C, and for durations between 0.5 and 92 hours. The detailed experimental conditions are listed in Table 1. The experiments were performed using a non-end-loaded piston-cylinder apparatus and a Boyd-England type piston-cylinder apparatus at the Magma Factory, Tokyo Institute of Technology (Takahashi et al. 1993). The experiments at 1375 °C were carried out with a 1/2 inch diameter furnace assembly including talc, a Pyrex glass outer sleeve, and an ALSIMG inner sleeve with a straight graphite heater. The large size heater (6 mm inner diameter and 0.75 mm in thickness) was chosen in this study for experiments using the three different capsules simultaneously. The experiments at 1425 °C were carried out with 3/4 inch-diameter assemblies using the same materials as the 1/2 inch furnace, with a tapered graphite heater (Kushiro 1976).

Pressures in the 1/2 inch furnace were calibrated using the albite ↔ jadeite + quartz reaction at 600 °C, 1.63 GPa (Holland 1980), the melting point of Au at 1150 °C, 1.5 GPa (Akella and Kennedy 1971), and the quartz ↔ coesite phase transition at 1000 °C, 2.97 GPa (Bohlen and Boettcher 1982). We estimated the pressure correction to be –16 ± 2% of the nominal piston pressure. The pressure loss by friction of the 3/4 inch furnace was estimated as approximately 7% (Takahashi, unpublished data). The temperature was measured and controlled by a W_5Re-$W_{26}Re$ thermocouple. No pressure correction was made on the emf of the thermocouple.

TABLE 1. Run conditions and results of experiments for evaluation of sample containers

Run no.	*P* (GPa)	*T* (°C)	Duration (hour)	Container	Products
AK18a	1.5	1375	5	Pt	ol+opx+cpx+sp+m
b	1.5	1375	5	Re/Pt	ol+opx+cpx+sp+m
c	1.5	1375	5	graphite/Pt	ol+opx+cpx+sp+m
AK19a	1.5	1375	1	Pt	ol+opx+cpx+sp+m
b	1.5	1375	1	Re/Pt	ol+opx+cpx+sp+m
c	1.5	1375	1	graphite/Pt	ol+opx+cpx+sp+m
AK21a	1.5	1375	0.5	Pt	ol+opx+cpx+sp+m
b	1.5	1375	0.5	Re/Pt	ol+opx+cpx+sp+m
c	1.5	1375	0.5	graphite/Pt	ol+opx+cpx+sp+m
AK22a	1.5	1375	20	Pt	ol+opx+cpx+sp+m
b	1.5	1375	20	Re/Pt	ol+opx+cpx+sp+m
c	1.5	1375	20	graphite/Pt	ol+opx+cpx+sp+m
AK23a	1.5	1375	10	Pt	ol+opx+cpx+sp+m
b	1.5	1375	10	Re/Pt	ol+opx+cpx+sp+m
c	1.5	1375	10	graphite/Pt	ol+opx+cpx+sp+m
AK24a	1.5	1425	5	Pt	ol+opx+sp(F)+m
b	1.5	1425	5	Re/Pt	ol+opx+sp+m
P299 a	1.5	1425	10	Pt	ol+opx+sp(F)+m
b	1.5	1425	10	Re/Pt	ol+opx+cpx+sp+m
c	1.5	1425	10	graphite/Pt	ol+opx+m
P300 a	1.5	1425	20	Pt	ol+opx+sp(F)+m
b	1.5	1425	20	Re/Pt	ol+opx+m
c	1.5	1425	20	graphite/Pt	ol+opx+m
P304 a	1.5	1425	92	Pt	ol+opx+sp(F)+m
b	1.5	1425	92	Re/Pt	ol+opx+m
c	1.5	1425	92	graphite/Pt	ol+opx+m
AK20a	1.5	1250	44.25	Pt	ol+opx+cpx+sp
b	1.5	1250	44.25	Re/Pt	ol+opx+cpx+sp
c	1.5	1250	44.25	graphite/Pt	ol+opx+cpx+sp

Notes: m = melt, ol = olivine, opx = orthopyroxene, cpx = clinopyroxene, sp = chromian spinel, sp(F) = Fe^{3+}-rich spinel.

Estimation of oxygen fugacities

The run products were sectioned longitudinally and polished for analysis. Minerals were analyzed by wavelength-dispersive spectrometers using an electron microprobe (JEOL-JXA8800) at the Tokyo Institute of Technology. Analytical conditions were 15kV accelerating voltage and 1.20×10^{-8}A beam current, with a ZAF correction procedure. Standards used were wollastonite for Si and Ca, rutile for Ti, corundum for Al, chromian spinel for Cr, hematite for Fe, periclase for Mg, albite for Na, K-feldspar for K, and nickel oxide for Ni. The oxygen fugacity of the run products was calculated from the equilibrium: $6Fe_2SiO_4$ (olivine) + O_2 = $3Fe_2Si_2O_6$ (opx) + 2 $Fe^{2+}Fe_2^{3+}$ O_4 (spinel), as described by Bryndzia and Wood (1990). The Fe^{3+}/Fe^{2+} ratios (magnetite component) of the spinel were calculated by assuming spinel stoichiometry. The activities of Fe_2SiO_4 (olivine) and $Fe_2Si_2O_6$ (opx) were estimated by the method of Mattioli and Wood (1988), and that of Fe_3O_4 (spinel) was calculated by the method of Wood et al. (1990).

Results

The Mg' of olivine is a good indicator of Fe loss from run products. The Fe loss from an experimental charge is increased by the existence of an Fe-bearing silicate melt because of its rapid reaction rate with the metal capsule. The composition of the glass quenched from melt at high pressure is, however, significantly modified by overgrowth of quenched crystals (olivine and pyroxenes). Liquidus pyroxene crystals had relict cores of starting material crystals if the run duration was less than about 20 hours. It was very difficult to estimate the bulk Fe loss for these reasons. Olivine did not show any compositional zoning except in quenched rims because the Mg' of olivine changes rapidly with the change in Mg' of the coexisting melt at high temperatures. Therefore, the Mg' of olivine is useful to evaluate the degree of the Fe-loss.

Figure 1 shows the change in the Mg' of olivine as a function of time. At 1375 °C, the degree of partial melting was less than 1 vol% and the olivine in the Pt single capsule showed highly variable Mg' from 0.900 at the center to 0.990 at the margin of the capsule. On the other hand, the Mg' of olivine in the Re/Pt capsule was homogeneous throughout the charge, and was the same as that in the graphite/Pt capsule. At 1425 °C, the degree of partial melting was about 16 vol% and the Mg' of olivine was different in the three capsule types, although there were no chemical and textural variations throughout the containers. The Mg' was about 0.910 in graphite/Pt, 0.917 in Re/Pt, and 0.945 in Pt for run durations of less than 20 hours. The degree of partial melting was estimated by point counting of back-scattered electron (BSE) images (1024 × 1024 points, 0.3–0.3 μm pixel size) combined with compositional maps for Na and Mg.

Platinum reacts readily with Fe and makes an alloy. The high Mg' at the margin of the Pt capsule at 1375 °C (Fig. 1a) indicates that both melt and solid next to the Pt capsule lost a significant proportion of their Fe. Iron loss did not occur effec-

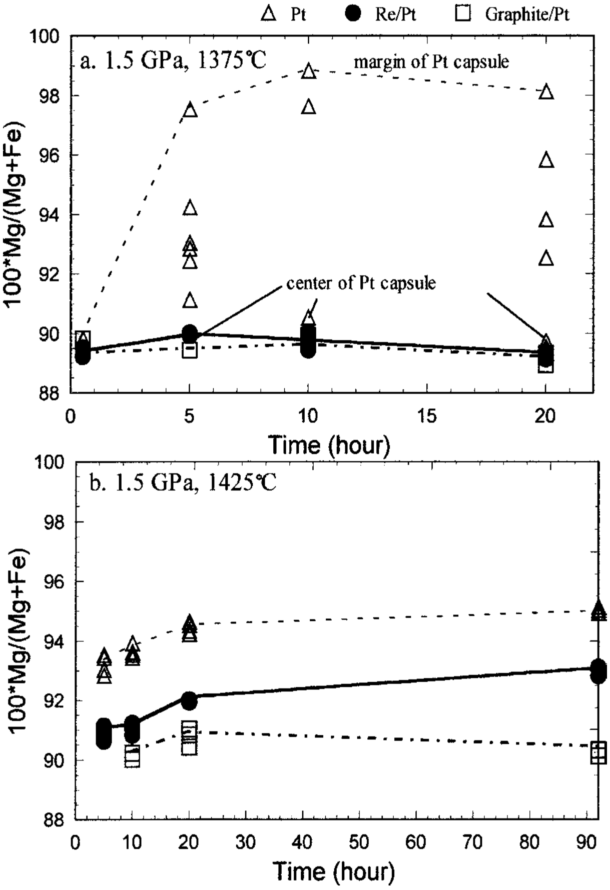

FIGURE 1. Change of the Mg' = [Mg/(Mg + Fe^{2+})] of olivine as a function of time. The Mg' of olivine in three different containers (Pt, Re/Pt, and graphite/Pt) is compared in order to assess their capability to minimize Fe loss (see text). Experiments were carried out at 1.5 GPa and 1375–1425 °C (see Table 1).

tively from the center of the capsule because the partial melt at the grain boundaries was not interconnected at such low degrees of partial melting. Compared to the sample in Pt, the sample in the Re/Pt double capsule did not show any Fe loss at 1375 °C. At 1425 °C, the melt network was completely formed and the Mg' of olivine was essentially homogeneous in each capsule. Iron loss to containers was recognized in both Pt and Re/Pt capsules at such high degrees of melting. The loss to the Pt capsule was especially high if the run duration was less than several hours. The Mg' of olivine in the Re/Pt capsule is clearly lower than that in Pt but is slightly higher than that in graphite/Pt capsule (Fig. 1b). These results thus demonstrate that the amount of Fe loss to the Re/Pt container is insignificant compared with Pt capsule at 1375–1425 °C. As shown later, however, the degree of Fe loss becomes serious, even in Re/Pt capsules at temperatures higher than about 1450 °C, as described by Bryndzia and Wood (1990).

Figure 2 shows the calculated delta FMQ [= log (f_{O_2})–log (FMQ)] of run products as a function of time. The delta FMQ in the Pt single capsule varied spatially at 1375 °C (Fig. 2a) because of the heterogeneity of mineral compositions described above (e.g., Fig. 1a). Delta FMQ values in Pt, Re/Pt, and graphite/Pt capsules were 2 to 8, –3 to 0, and <–5, respectively (Figs. 2a and 2b). The shaded area of Figure 2 represents the range of f_{O_2} of mantle-derived natural peridotites [mantle xenoliths (Mattioli and Wood 1986), a mantle section of the Oman ophiolite, East Pacific Rise peridotites, and Horoman peridotites (Matsukage unpublished data)]. The oxygen fugacity of the uppermost mantle has been estimated to be about that of the FMQ buffer (e.g., Mattioli and Wood 1986). The run product in the Pt single capsule was highly oxidized compared with the natural peridotites. On the other hand, the use of the graphite/Pt capsule imposed a low f_{O_2} on the sample, and spinel readily disappeared at 1425 °C (Table 1) due to its highly reduced condition. In the Re/Pt capsule, spinel existed at 1425 °C in experiments when the duration was less than 10 hours, whereas spinel always disappeared in longer runs (see Table 1). The stability of spinel is related to the chemistry of the coexisting orthopyroxene. For short run durations, almost all of the orthopyroxene (approximately 10 μm in diameter) had relic cores of Al-rich, Cr- and Mg-poor starting material. This observation indicates that chromian spinel is chemically unstable under these conditions (1.5 GPa, 1425 °C). In our study, oliv-

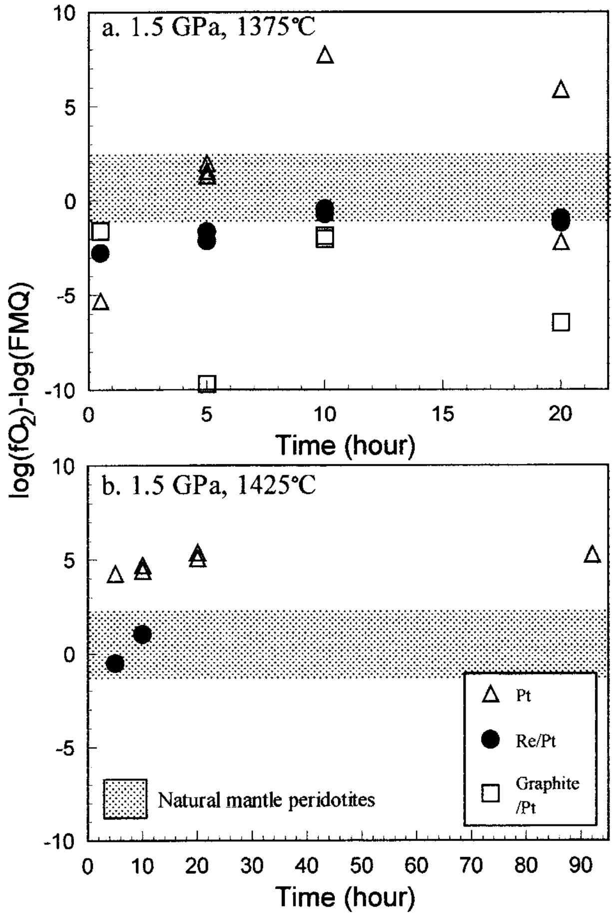

FIGURE 2. Calculated delta FMQ [= log (f_{O_2}) – log (FMQ)] of run products in Pt, Re/Pt, and graphite/Pt capsules as a function of time. The range of delta FMQ of natural mantle peridotites (spinel lherzolite and spinel harzburgite) is after Bryndzia and Wood (1990). Experiments were carried out at 1.5 GPa and 1375–1425 °C (see Table 1).

ine and orthopyroxene in contact with spinel were chosen for calculations of f_{O_2} because local chemical equilibrium may be achieved among these minerals. The f_{O_2} of the sample in the Re/Pt capsule was calculated to be very close to FMQ buffer at both 1375 and 1425 °C (Fig. 2).

Figure 3 shows the atomic ratios of Fe^{3+}, Cr, and Al in spinels at the centers of the sample containers. $Fe^{3+}/(Fe^{3+} + Al + Cr)$ atomic ratios were related to the variation of container materials and run durations of different experiments. Most spinels from natural spinel lherzolite and harzburgite contain a small amount of an Fe_2O_3 component. Their $Fe^{3+}/(Fe^{3+} + Al + Cr)$ atomic ratios generally range from 0.01 to 0.1. In the experiments at 1375 °C, $Fe^{3+}/(Fe^{3+} + Al + Cr)$ atomic ratios of spinels in Re/Pt capsules were between 0.01 and 0.1. These values agree with those of natural mantle peridotites (stippled area of Fig. 3). The $Fe^{3+}/(Fe^{3+} + Al + Cr)$ atomic ratios of spinels in the graphite/Pt capsule, however, were almost 0 due to the very reducing conditions imposed by the graphite. The oxygen fugacity in the graphite/Pt container of our experiments would be close to the IW buffer (Mattioli and Wood 1986). Takahashi and Kushiro (1983) discussed how the low oxygen fugacity in the presence of graphite causes reduction of Cr^{3+} to Cr^{2+}, which dissolves in olivine and pyroxenes instead of spinel and, therefore, make the spinel stability field significantly narrower. In Pt capsules, the $Fe^{3+}/(Fe^{3+} + Al + Cr)$ atomic ratios of spinel increased up to 0.25, with increasing temperature (1425 °C) and degree of partial melting. The spinel chemistry also indicates that the run charge in the Pt single capsule is highly oxidized. Roeder and Reynolds (1991) documented the large decrease of Cr solubility in chromian spinel-saturated basaltic melts as a function of increasing f_{O_2} in experiments at 1 atm at f_{O_2} values close to FMQ buffer. The wide stability field of spinel in our experiments using Pt single capsules, in contrast to those using graphite/Pt and Re/Pt capsules (see Table 1), is caused by the oxidization during formation of a Pt-Fe alloy from Pt and FeO.

Borisov and Jones (1999) conducted experiments using an f_{O_2} controlling, 1 atm furnace for evaluation of the Re loop as a sample container for Fe-bearing melts. They concluded that the experiments using Re of several days duration were possible at a temperature of 1400 °C and an f_{O_2} of FMQ-2. The Fe loss was highly reduced (less than 1 wt%) and decreased with increasing f_{O_2}. The result of their experiments at a pressure of 1 atm agrees well with that of our experiments at 1.5 GPa. Our study using the Re/Pt capsule appears to produce the desired effect, such as elimination of Fe loss at about FMQ at high-pressure and high–temperature. Accordingly, the Re/Pt capsule is found to be the most suitable sample container for conducting melting experiments on dry peridotite at the proper oxygen fugacity of the terrestrial uppermost mantle.

EXPERIMENT FOR CHROMIAN SPINEL STABILITY AND CHEMISTRY

Experimental conditions

Using the Re/Pt capsule, melting experiments of KLB-1 were conducted at pressures between 1.0 and 2.5 GPa and temperatures between 1250 and 1500 °C. The phase relations and spinel compositions were determined by the method described above. The experimental conditions and phase relations are listed in Table 2.

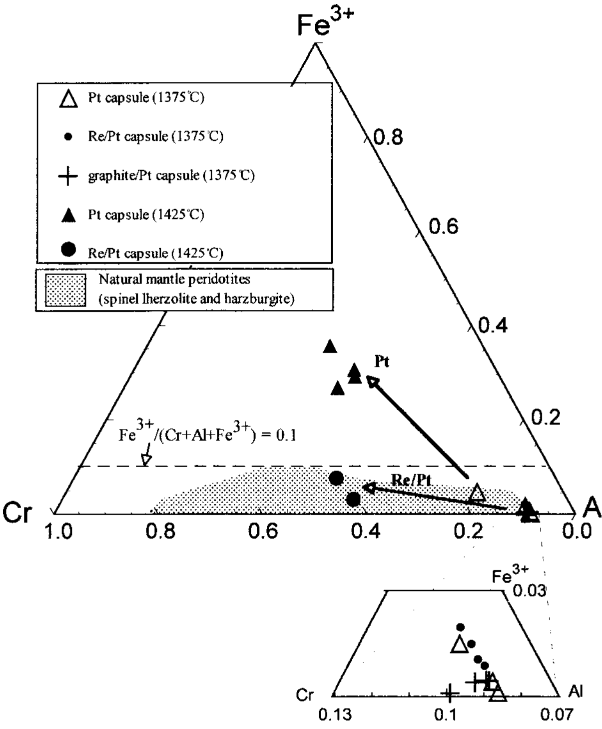

FIGURE 3. Chromian spinel compositions of run products in the three sample containers (Pt, Re/Pt, and graphite/Pt). The range of spinel compositions in natural mantle peridotites (lherzolite and harzburgite) is after Figure. 6 in this paper. Experiments were carried out at 1.5 GPa and 1375–1425 °C (see Table 1).

Results

A phase diagram for melting of dry KLB-1 is shown in Figure 4. Chromian spinel chemistry is listed in Table 3. The subsolidus assemblage between 1.0 to 2.5 GPa is olivine + orthopyroxene + clinopyroxene + spinel, and above 2.5 GPa is olivine + orthopyroxene + clinopyroxene + garnet (Table 2). The dry solidus of KLB-1 lherzolite shown in Figure 4 is after Takahashi et al. (1993), and is concordant with the solidus of our study. Above the dry solidus, clinopyroxene was preferentially melted relative to olivine and orthopyroxene with increasing temperature. Therefore, the residual rock type changed from lherzolite to harzburgite (without clinopyroxene). The upper-temperature stability of clinopyroxene increased in temperature with increasing pressure in the same manner as the solidus line (Fig. 4). The spinel-out line, however, decreased and then increased (Fig. 4). The stability of spinel is highly influenced by the solubility of Al and Cr in coexisting pyroxenes and partial melt. The concentration of Al in pyroxenes of high pressure (1.5 and 2.0 GPa) was higher than that of low pressures (1.0 GPa). For example, the Al_2O_3 concentration of clinopyroxene was 6.5–5.4 wt% at 1300–1380 °C, 1.0 GPa, and 8.1–7.5 wt% at 1350–1390 °C, 1.5 GPa, respectively. In other word, the spinel that is a reservoir of Al at 1.0 GPa dissolved effectively in pyroxenes at above 1.5 GPa. As a result, the stability field of spinel first shrank then was constant toward higher pressure. Specifically, chromian spinel disappeared

TABLE 2. Run conditions and results of melting experiments of KLB-1 with Re/Pt capsules

Run no.	*P* (GPa)	*T* (°C)	Duration (hour)	Run products
AK31	1.0	1250	72	ol+opx+cpx+sp
AK30	1.0	1300	48	ol+opx+cpx+sp
AK27	1.0	1350	20	ol+opx+cpx+sp+m
AK43	1.0	1380	20	ol+opx+cpx+sp+m
AK44	1.0	1420	20	ol+opx+sp+m
AK67	1.0	1430	15	ol+opx+m
AK33	1.0	1450	10	ol+opx+m
AK45	1.0	1500	10	ol+opx+m
AK20b	1.5	1250	44.2	ol+opx+cpx+sp
P348	1.5	1350	25	ol+opx+cpx+sp
AK22b	1.5	1375	20	ol+opx+cpx+sp+m
P350	1.5	1390	24	ol+opx+cpx+sp+m
P341	1.5	1400	20	ol+opx+m
P300b	1.5	1425	20	ol+opx+m
P311	1.5	1450	17	ol+opx+m
P317	1.5	1490	20	ol+opx+m
P371	2.0	1400	20	ol+opx+cpx+sp+m
P431	2.0	1430	20	ol+opx+cpx+sp+m
P374	2.0	1450	20	ol+opx+m
P338	2.5	1410	20	ol+opx+cpx+grt
P319	2.5	1450	25	ol+opx+cpx+grt+m
P320	2.5	1490	24	ol+opx+m

Notes: m = melt, ol = olivine, opx = orthopyroxene, cpx = clinopyroxene, sp = spinel, grt = garnet.

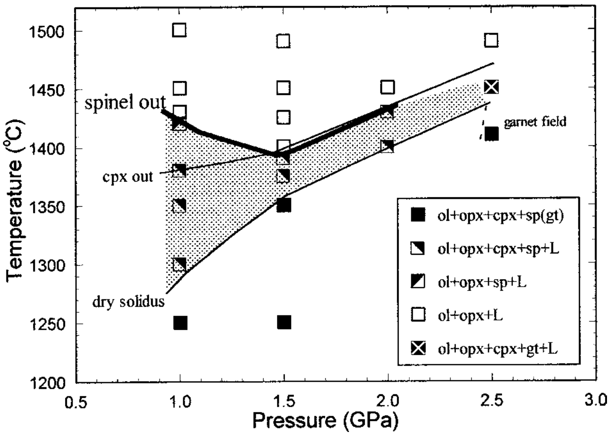

FIGURE 4. Melting phase relations of dry spinel lherzolite (KLB-1). The experiments were conducted using a Re/Pt capsule. Stippled area indicates the chromian spinel stability field above the solidus.

TABLE 3. Chemical compositions of spinel and calculated oxygen fugacities in delta FMQ [= log (f_{O_2}) – log (FMQ)] of experiments using Re/Pt capsule

Run no.	n*	SiO_2	TiO_2	Al_2O_3	Cr_2O_3	FeO*	MgO	NiO	Total	Mg'	(1σ)	Cr'	(1σ)	Fe^{3+}/ (Fe^{3+}+Al+Cr)	(1σ)	delta FMQ	degree of melting (vol%)
AK31	5	1.56	0.16	57.52	8.51	9.33	21.43	0.36	98.87	0.804	(0.013)	0.090	(0.002)	0.020	(0.005)	–0.24	0
AK30	4	3.30	0.18	49.47	12.13	12.18	23.10	0.40	100.76	0.772	(0.002)	0.141	(0.011)	0.093	(0.013)	1.51	<1
AK27	1	1.50	0.19	51.15	14.41	8.78	23.57	0.29	99.89	0.827		0.159		0.056		0.26	9
AK43	6	1.55	0.12	40.28	26.09	9.86	20.30	0.21	98.41	0.789	(0.008)	0.303	(0.036)	0.040	(0.002)	0.07	18
AK44	3	0.29	0.12	32.08	34.78	10.61	19.15	0.19	97.22	0.763	(0.006)	0.421	(0.036)	0.045	(0.002)	0.50	23
AK20b	8	0.11	0.16	59.34	8.69	9.44	21.28	0.23	99.25	0.819	(0.005)	0.089	(0.003)	0.008	(0.002)	–1.79	0
P348	6	0.29	0.22	59.48	8.50	10.20	21.71	0.37	100.77	0.827	(0.002)	0.087	(0.002)	0.018	(0.001)	–0.76	0
AK22b	6	0.23	0.12	58.83	8.46	9.51	21.56	0.32	99.03	0.831	(0.005)	0.088	(0.002)	0.016	(0.002)	–0.81	<1
P350	8	0.62	0.15	57.05	10.41	10.61	21.67	0.41	100.91	0.832	(0.009)	0.109	(0.008)	0.027	(0.004)	–0.13	12
P371	1	4.38	0.31	52.45	8.67	8.33	22.18	0.36	96.68	0.826		0.100		0.048		–0.10	<1
P431	1	0.29	0.16	55.24	12.70	8.95	21.36	0.39	99.09	0.836		0.134		0.013		–1.18	2

Notes: Mg' = Mg/(Mg + Fe^{2+}) atomic ratio, Cr' = Cr/(Cr + Al), Fe^{3+}/ = Fe^{3+}/(Fe^{3+} + Al + Cr), (σ) = one standard deviation.
* Number of analyes.

at low degrees of melting above 1.5 GPa in our experiments (Table 3). These results are quite different from previous studies that used Pt capsules (e.g., Jaques and Green 1980), graphite/Pt capsule (e.g., Takahashi 1986), and graphite capsule (e.g., Falloon et al., 1999).

The relative amounts of trivalent cations of chromian spinel are shown in Figure 5. Analyzing several spinel crystals in run products checked analytical reproducibility. The number of analyzed points and statistical uncertainties (one standard deviation) for $Fe^{3+}/(Fe^{3+} + Al + Cr)$ atomic ratio, Cr', and Mg' are listed in Table 3. The $Fe^{3+}/(Fe^{3+} + Al + Cr)$ atomic ratios of spinels in our study lie between 0.05 and 0.1, and are not systematically related to pressure or temperature (Table 3). The variation of trivalent cations is similar to the natural trend of lherzolite and harzburgite (Fig. 6). Calculated oxygen fugacity values of our melting experiments range between –1.18 and 1.51 log units from the FMQ buffer (Table 3). These values are close to that of mantle-derived natural spinel-lherzolite and harzburgite (see shaded area in Fig. 2).

The Cr' of liquidus chromian spinel has a positive correlation with the degree of melting (Table 3; Fig. 7). The upper limit of the Cr' of spinel, just before its disappearance, decreases rapidly with increasing pressure. The upper limit of the Cr' is 0.43, 0.12, and 0.13 at 1.0, 1.5, and 2.0 GPa respectively. The Mg' of spinel has a negative correlation with the Cr' (Fig. 8).

Implications on petrogenesis of abyssal peridotites

The compositional variations of chromian spinel in natural mantle peridotites as a function of changing lithology have been well-documented with many field observations. Figures 6 and 8 show the spinel compositions in lherzolite and harzburgite from known tectonic settings. There are two important features of chromian spinel from terrestrial uppermost mantle. The first is that spinel exists in nearly all facies (lherzolite and harzburgite) of all tectonic settings. The second is its wide range in Cr's, which generally increase from 0.1 to 0.6, reaching 0.8 in some cases (Fig. 6). The systematic variations in the Cr' of spinel with indicators of the depletion of peridotite (e.g., con-

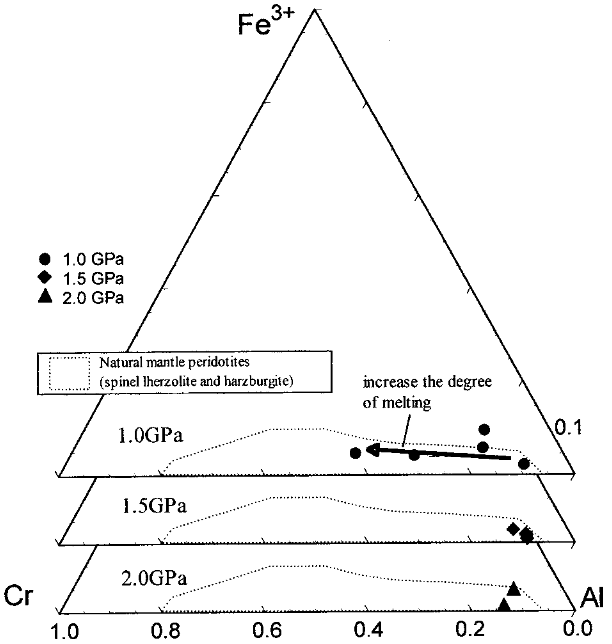

FIGURE 5. Chromian spinel compositions of run products using Re/Pt capsule. The experimental conditions are listed in Table 2. The range of natural mantle peridotites (spinel lherzolite and spinel harzburgite) is after Figure 6 in this paper.

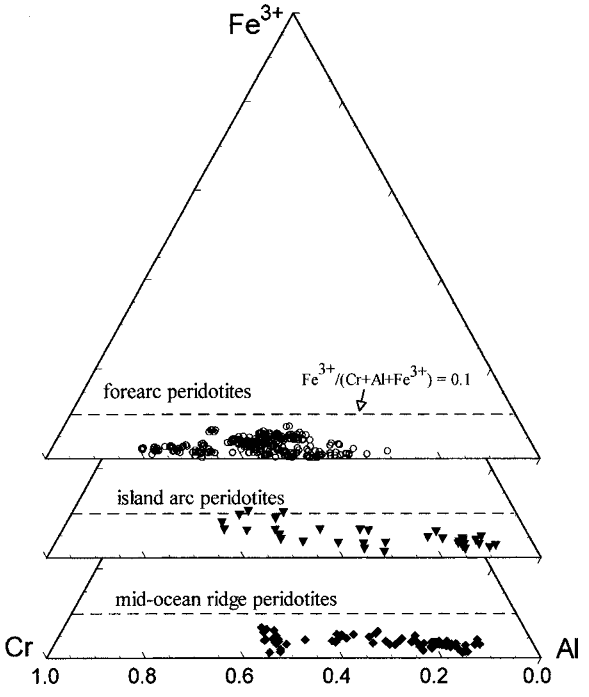

FIGURE 6. Compositions of chromian spinels in natural mantle peridotites (spinel lherzolite and spinel harzburgite) from various tectonic settings. Data for the forearc (Conical and Torishima seamounts) are after Ishii et al. (1992). Data for the island arcs (Japan arc, Luson arc, and Kamchatka arc) are after Abe et al. (1998, 1999) and Arai and Kida (2000). Data for the mid-ocean ridges (America-Antarctic Ridge, Southwest Indian ridge and East pacific Rise) are after Dick (1989), Arai and Matsukage (1996), and Dick and Natland (1996).

centration of some incompatible elements and modal proportion of clinopyroxene) have been discussed by many authors (Dick and Bullen 1984; Dick 1989; Arai 1989; Dick and Natland 1996; Takahashi 1992; Matsukage and Arai 1997; Ozawa 1997). The petrological variations from lherzolite to harzburgite are considered to have resulted from partial melting and melt-extraction processes, and the Cr' of spinel is considered to be a good indicator of degree of partial melting within the spinel stability field.

An important difference was observed, however, between our experiments and natural peridotites in the stability field and Cr' of chromian spinel. Spinel, which is common in natural peridotite, disappeared immediately at low degrees of melting in our experiments. Figures 5, 6, and 8 compare the chemical composition of the spinel obtained in our experiment with those observed in natural peridotites. It is clear that none of the chemical variations in natural chromian spinel, regardless of their tectonic settings, can be reproduced by anhydrous batch melting experiments at pressures more than 1.0 GPa.

Peridotites from mid-ocean ridges have been considered as good examples of restites derived from the uppermost mantle, and the upper limit to the Cr' of their constituent spinels is about 0.6 (Figs. 6 and 8). The chemical trend of chromian spinel from peridotites with Cr-poor spinel (lherzolite) to that with Cr-rich spinel (harzburgite) has been interpreted as a result of simple partial melting and melt extraction processes (e.g., Dick and Bullen 1984; Dick 1989). In this case, the maximum Cr' of spinel in abyssal peridotites should correspond with the maximum degree of partial melting at the MOR. If the abyssal peridotites are the simple residue of batch partial melting at MORs, the high maximum Cr' of their spinels (about 0.5–0.6) must indicate that the degree of partial melting exceeds 25% and clinopyroxene must have been exhausted in all of them (e.g., Ozawa 1997). This conclusion is not consistent with some geochemical observations. In harzburgites containing spinel with a high Cr', the concentrations of incompatible trace elements (e.g., LREE, MREE, Ti, Zr) are extremely low compared with those expected theoretically in restite formed by 25% batch partial melting (Johnson et al. 1990; Dick and Natland 1996). The remarkable depletion in the abyssal peridotites from some MORs indicate that they were not formed by batch melting but by melting and segregation in <0.1% increments (incremental melting; Johnson et al. 1990). Incremental melting is defined as the melting process of multi-step batch melting and melt segregation, in other word, the process is a combination of batch and fractional melting. If this conclusion is correct, the upper limit of melting is inferred to be constrained by the disappearance of clinopyroxene during incremental melting processes; more melt cannot be produced until much higher temperatures, beyond the solidus of harzburgite (e.g., Presnall 1969). This idea is supported by the observation that in some of the harzburgites containing spinel with the highest Cr', clinopyroxene has almost disappeared, and some harzburgites do not contain any clinopyroxene at all.

Our experimental results show a strong pressure dependence on the upper limit of the Cr' in spinel during anhydrous batch melting at pressures less than 1.5 GPa. In other words, the Cr' of spinel equilibrated with lower-pressure melts is higher than that with higher-pressure melt for given degree of melting (Fig.

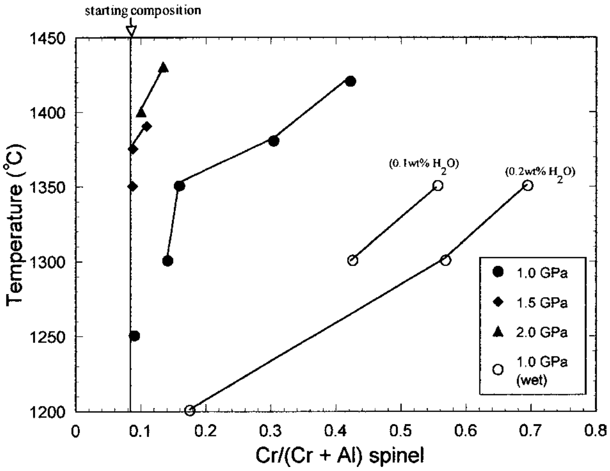

FIGURE 7. The variation in Cr' of chromian spinel with changing temperature and amount of H_2O in KLB-1 lherzolite. Hydrous data are after Hirose and Kawamoto (1995).

7). Consequently, it is difficult for harzburgite containing spinel with an intermediate Cr' (about 0.4–0.6) to be the product of batch partial melting at any pressure above 1.0 GPa. The most depleted abyssal peridotites must be the restite from incremental melting because incremental melting processes can more effectively concentrate the compatible elements (e.g., Cr) into the solid relative to the batch-melting process. The expansion of the stability field of spinel at lower pressure (see Fig. 4) implies that the abyssal peridotites can be produced by a few episodes of melt segregation if the partial melting occurs at low pressure, and the "batch-melting mode" in incremental melting becomes the dominant process. Thus, some abyssal peridotites could be residues after batch partial melting if the melting occurred at lower pressures (less than 1.0 GPa), whereas those with high Cr' spinels could be restite after incremental melting at higher pressure (more than 1.0 GPa) at MORs.

Implication on genesis of other peridotites

Harzburgite containing spinels with Cr' > 0.4 are common occurrences in arc and forearc regions (Figs. 6 and 8; Arai 1987; Ishii et al. 1992; Abe et al. 1998; Arai and Kida 2000). The Cr' of spinels from these tectonic setting reaches 0.8 in some cases. The arc and forearc peridotites are characterized by a wide variation in the Cr' of spinel (see Fig. 8). In subduction zones, it is generally believed that some amount of water is transported to the wedge mantle by subducted hydrous crust and mantle. Therefore, the influence of water has to be taken into account when considering the origin of mantle peridotites from arc and forearc regions. In fact, the concentrations of some incompatible components in residual clinopyroxene that are highly mobile in water (e.g., Ce, Sr, and Zr; Kogiso et al. 1997) increase dramatically with the Cr' of spinel and decrease with the modal proportion of clinopyroxene in arc and forearc peridotites (e.g., Abe et al. 1998). These observations imply that the partial melting is stimulated by flux melting induced by an H_2O-rich melt (or fluid) released by dehydration of subducted crust and mantle.

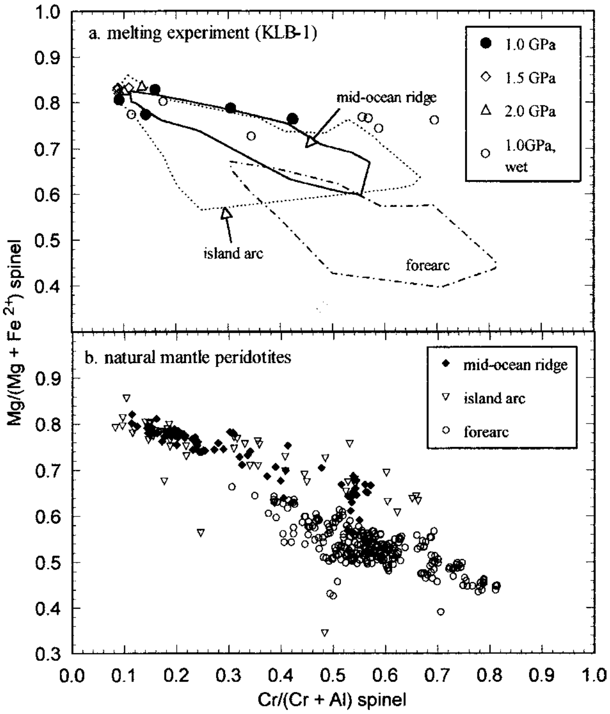

FIGURE 8. Relationship between the Cr' and the Mg' of chromian spinel. (**a**) Melting experiments of dry and slightly hydrous (<0.9 wt% H_2O) KLB-1. Hydrous data are after Hirose and Kawamoto (1995). (**b**) Natural mantle peridotites (spinel lherzolite and harzburgite). Data for the forearc (Conical and Torishima seamounts) are after Ishii et al. (1992). Data for the island arcs (Japan arc, Luson arc and Kamchatka arc) are after Abe et al. (1998, 1999) and Arai and Kida (2000). Data for the mid-ocean ridges (America-Antarctic Ridge, Southwest Indian ridge and East Pacific Rise) are after Dick (1989), Arai and Matsukage (1996) and Dick and Natland (1996).

To examine the effect of H_2O on liquidus spinel chemistry, experimental results of hydrous melting of KLB-1 lherzolite (Hirose and Kawamoto 1995) were compared with the results of our anhydrous experiments at 1.0 GPa (Figs. 7 and 8). The oxygen fugacity of their experiments, estimated by the method of this study, is about FMQ + 1 to + 2. Therefore, oxygen fugacity in their charges was close to that of the terrestrial upper mantle, as well as that of our experiments. Figure 8a shows the relation between Cr' and Mg' of spinel in both sets of experiments. The Cr' and Mg' of spinels are negatively correlated and the slope is independent of the H_2O contents. The experiments show that the upper limit to the Cr' of spinel clearly increases with increasing H_2O for a given degree of melting (Fig. 7). This result implies that the Al-Cr partition coefficient between spinel and melt changes with melt composition and that chromian spinel can easily survive in hydrous conditions. Alternatively, refractory harzburgite, which contains chromian spinel with a high Cr', formed only at extra-high temperatures in dry conditions but is stable in hydrous conditions at relatively low temperatures (Fig. 7). Based on these experiments, we suggest that harzburgite with Cr-rich spinel (Cr' > 0.4) may exist universally in the hydrous mantle wedge.

The H_2O-rich melt (fluid) phase is buoyant and will migrate upwards, thus becoming separated from residual minerals. Therefore, the melting process under hydrous conditions is considered to be an open system (influx melting with segregation in small increments). For this reason, batch melting experimental data are not directly comparable with natural arc and forearc peridotites. However, that the stability field of Cr-rich spinel increases under hydrous conditions has very important implications for the origin of arc and forearc harzburgites with Cr-rich spinel. The expansion of the spinel stability field also may be responsible for the close relationship between hydrous mineral inclusions and spinel concentrations in mantle peridotites and chromitite (e.g., Johan et al. 1980; Matsukage and Arai 1997). The characteristics of spinel in the melting experiments supports the hypothesis that arc and forearc peridotites have evolved by melting with an influx of H_2O-bearing fluid or melt.

ACKNOWLEDGMENTS

We are greatly indebted to E. Takahashi and P. Smith for discussion and critical reading of the early drafts. We thank E. Takahashi, K. Hirose, K. Nakajima, M. Shirasaka, and Y. Nishihara for their advice in experimental techniques. Critical reviews and helpful comments on our earlier manuscript by R.F. Dymek and D.C. Presnall are highly appreciated. K.N.M. is grateful for the Research Fellowships of the Japan Society for the Promotion of Science for Young Scientists.

REFERENCES CITED

Abe, N., Arai, S., and Yurimoto, H. (1998) Geochemical characteristics of the uppermost mantle beneath the Japan island arcs: implications for upper mantle evolution. Physics of the Earth and Planetary Interiors, 107, 233–248.

——— (1999) Texture-dependent geochemical variations of sub-arc mantle peridotite from Japan island arcs. 7th Kimberlite Conference Proceedings, 13–22.

Akella, J. and Kennedy, G.C. (1971) Melting of Gold, Silver, and Copper—Proposal for a new high-pressure calibration scale. Journal of Geophysical Research, 76, 4969–4977.

Arai, S. (1987) An estimation of the least depleted spinel peridotite on the basis of olivine-spinel mantle array. Neues Jahrbuch fur Mineralogie, Monatshefte, 8, 347–354.

———(1994) Characterization of spinel peridotites by olivine-spinel compositional relationships: Review and interpretation. Chemical Geology, 113, 191–204.

Arai, S. and Kida, M. (2000) Origin of fine-grained peridotite xenoliths from Iraya volcano of Batan Island, Philippines: deserpentinization or metasomatism at the wedge mantle beneath an incipient arc? The Island Arc, 9, 458–471.

Arai, S. and Matsukage, K. (1996) Petrology of the gabbro-troctolite-peridotite complex from Hess Deep, equatorial Pacific: implications for mantle-melt interaction within the oceanic lithosphere. Proceedings of the Ocean Drilling Program, Scientific Results, 147, 135–155.

Bohlen, S.R. and Boettcher, A.L. (1982) The Quartz´Coesite Transformation: A Precise Determination and the Effects of Other Components. Journal of Geophysical Research 87, 7073–7078.

Borisov, A. and Jones, J.H. (1999) An evaluation of Re, as an alternative to Pt, for the 1 bar loop technique: An experimental study at 1400 °C. American Mineraligist, 84, 1528–1534.

Bryndzia, L.T. and Wood, B.J. (1990) Oxygen thermobarometry of abyssal spinel peridotites: the redox state and C-O-H volatile composition of the earth's sub-oceanic upper mantle. American Journal of Science, 290, 1093–1116.

Dick, H.J.B. (1989) Abyssal peridotite, very slow spreading ridges and ocean ridge magmatism. Geological Society Special Publication, 42, 72–105.

Dick, H.J.B. and Bullen, T. (1984) Chromian spinel as a petrogenetic indicator in abyssal and alpine-type peridotites and spatially associated lavas. Contributions to Mineralogy and Petrology, 86, 54–76.

Dick H.J.B. and Natland, J.H. (1996) Late-stage melt evolution and transport in the shallow mantle beneath the East Pacific Rise. Proceedings of the Ocean Drilling Program, 147, 103–134.

Falloon, T.J., Green, D.H., Danyushevsky, L.V., and Faul, U.H. (1999) Peridotite melting at 1.0GPa: an experimental evaluation of techniques using diamond aggregates and mineral mixes for determination of near-solidus melts. Journal of Petrology, 40, 1343–1375.

Gaetani G.A. and Grove, T.L. (1998) The influence of water on melting of mantle peridotite. Contributions to Mineralogy and Petrology, 131, 323–346.

Hirose, K. and Kawamoto, T. (1995) Hydrous partial melting of lherzolite at 1GPa: the effect of H_2O on the genesis of basaltic magmas. Earth and Planetary Science Letter, 463–473.

Hirose, K. and Kushiro, I. (1993) Partial melting of dry peridotites at high pressures: Determination of compositions of melts segregated from peridotite using aggregates of diamond. Earth and Planetary Science Letter, 477–489.

Holland, T.J.B. (1980) The reaction albite = jadeite + quartz determined experimentally in the range 600–1200°C. American Mineralogist, 65, 129–134.

Ishii, T., Robinson, P.T., Maekawa, H., and Fiske, R. (1992) Petrological studies of peridotites from diapiric serpentinite seamounts in the Izu-Ogasawara-Mariana forearc. Proceedings of the Ocean Drilling Program, Scientific, 125, 445–485.

Jaques, A.L. and Green, D.H. (1980) Anhydrous melting of peridotite at 0-15 kb pressure and the genesis of tholeiitic basalts. Contributions to Mineralogy and Petrology, 73, 287–310.

Johan, Z., Dunlop H, Le Bel, L., Robert, J.L., and Volfinger, M. (1980) Origin of chromite deposits in ophiolite complex: evidence for a volatile and sodium-rich reducing fluid phase. Fortschritte der Mineralogie, 61, 105–107.

Johnson, K.T.M, Dick, H.J.B., and Shimizu, N. (1990) Melting in the oceanic upper mantle: an ion microprobe study of diopsides in abyssal peridotites. Journal of Geophysical Research, 95, 2661–2678.

Kawamoto, T. and Hirose, K. (1994) Au-Pd sample containers for melting experiments on iron and Water bearing systems. European Journal of Mineralogy, 6, 381–385.

Kogiso, T., Tatsumi, Y., and Nakano, S. (1997) Trace element transport during dehydration processes in the subducted oceanic crust: 1. Experiments and implications for the origin of oceanic island basalts. Earth and Planetary Science Letter, 148, 193–206.

Kogiso, T., Hirose, K., and Takahashi, E. (1998) Melting experiments on homogeneous mixtures of peridotite and basalt: application to the genesis of ocean island basalts. Earth and Planetary Science Letter, 162, 45–61.

Kubo, K. (2002) Dunite formation processes in highly depleted peridotite: Case study of the Iwanaidake peridotite, Hokkaido, Japan. Journal of Petrology, 43, 423–448.

Kushiro, I. (1976) A new furnace assembly with a small temperature gradient in solid-media, high-pressure apparatus. Carnegie Institution of Washington, Year Book, 75, 832–833.

Matsukage, K., and Arai, S. (1997) Ochiai-Hokubo peridotite and Horoman peridotite: a genetical comparison for insight into diverse melting processes in the upper mantle. The Memoirs of the Geological Society of Japan, 47, 173–183 (Japanese with English abstract).

——— (1998) Jadeite, albite and nepheline as inclusions in spinel of chromitite from Hess Deep, equatorial Pacific: their genesis and implications for serpentinite diapir formation. Contributions to Mineralogy and Petrology, 131, 111–122.

Mattioli, G.S. and Wood, B.J. (1986) Upper mantle oxygen fugacity recorded by spinel lherzolites. Nature, 322, 626–628.

——— (1988) Magnetite activities across the MgAl2O4-Fe2O4 spinel join, with application to thermobarometric estimates of upper mantle oxygen fugacity. Contributions to Mineralogy and Petrology, 98, 148–162.

Ozawa, K. (1997) Mechanism of magma generation constrained by mantle peridotites: Solid-dominant open magma system. Bulletin of the Volcanological Society of Japan 42, special number 'Magmalogy', S61–S85 (Japanese with English abstract).

Ozawa, K. and Shimizu, N. (1995) Open-system melting in the upper mantle: Constraints from the Hayachine-Miyamori ophiolite, northeastern Japan. Journal of Geophysical Research, 100, 22315–22335.

Presnall, D.C. (1969) The geometrical analysis of partial fusion, American Journal of Science, 267, 1178–1194.

Roeder, P.L. and Reynolds, I. (1991) Crystallization of chromite and chromium solubility in basaltic melts. Journal of Petrology, 32, 909–934.

Takahashi, E. (1986) Melting of a dry peridotite KLB-1 up to 14 GPa: implications on the origin of peridotitic upper mantle. Journal of Geophysical Research 91, 9367–9382.

Takahashi, E., Shimazaki, T., Tsuzaki, Y. and Yoshida, H. (1993) Melting study of a peridotite KLB-1 to 6.5 GPa and the origin of basaltic magmas. Phil. Trans. R. Soc. Lond. A, 342, 105–120.

Takahashi, E., Nakajima, K., and Wright, T.L. (1998) Origin of the Columbia River basalts: melting model of a heterogeneous plume head. Earth and Planetary Science Letter, 162, 63–80.

Takahashi, N. (1992) Evidence for melt segregation towards fractures in the Horoman mantle peridotite complex. Nature, 359, 52–55.

Walter, M.J. (1998) Melting of garnet peridotite and the origin of Komatiite and depleted lithosphere. Journal of Petrology, 39, 29–60.

Wood, B.J., Bryndzia, L.T. and Johnson, K.E. (1990) Mantle oxidation state and its relationship to tectonic environment and fluid speciation. Science, 248, 337–345.

MANUSCRIPT RECEIVED JUNE 24, 2002
MANUSCRIPT ACCEPTED APRIL 12, 2003
MANUSCRIPT HANDLED BY ROBERT DYMEK